Feedback Control of a Solid-State Qubit Using High-Fidelity Projective Measurement

D. Ristè, C. C. Bultink, K. W. Lehnert, and L. DiCarlo

Feedback control of a solid-state qubit using high-fidelity projective measurement

D. Ristè,[1] C. C. Bultink,[1] K. W. Lehnert,[2] and L. DiCarlo[1]

[1] *Kavli Institute of Nanoscience, Delft University of Technology,*
P.O. Box 5046, 2600 GA Delft, The Netherlands
[2] *JILA, National Institute of Standards and Technology and the University of Colorado and Department of Physics,*
University of Colorado, Boulder, Colorado 80309, USA

We demonstrate feedback control of a superconducting transmon qubit using discrete, projective measurement and conditional coherent driving. Feedback realizes a fast and deterministic qubit reset to a target state with 2.4% error averaged over input superposition states, and allows concatenating experiments more than 10 times faster than by passive initialization. This closed-loop qubit control is necessary for measurement-based protocols such as quantum error correction and teleportation.

Many protocols in quantum information processing (QIP) require closing a feedback loop where coherent control of qubits is conditioned on projective measurements in real time [1]. Important examples include quantum error correction and teleportation [2], so far achieved in ion-trap [3, 4] and photonic systems [5, 6]. During the last decade, the steady development of qubit readout and universal gates needed in a quantum processor [7] has made superconducting circuits [8] a leading solid-state QIP platform. However, the simple quantum algorithms [9] and teleportation-like protocol [10] so far demonstrated fall in the category of open-loop control. Measurement is performed as the final step, following a programmed sequence of applied gates. A comparable realization of closed-loop control has been precluded by stringent requirements on high measurement fidelity and short loop delay (latency). Until recently, the available qubit coherence times bottlenecked both achievable fidelity and required speed.

For feedback control of superconducting qubits, the development of circuit quantum electrodynamics [11, 12] with 3D cavities (3D cQED) [13] constitutes a watershed. The new order of magnitude in qubit coherence times ($> 10~\mu$s), combined with Josephson parametric amplification [14, 15], allows boosting projective-readout fidelity up to 98% [16, 17] and realizing feedback with off-the-shelf electronics. Very recently, feedback based on continuous weak measurement has sustained Rabi oscillations of a transmon qubit indefinitely [18]. Previously, this type of feedback had only been used to generate and stabilize quantum states of photons [19], ions [20], and atoms [21].

In this Letter, we demonstrate feedback control of a superconducting transmon qubit based on discrete, projective measurement. This dual type of feedback is the kind necessary for measurement-based QIP. As a first application, we demonstrate a feedback-based reset that is deterministic and fast compared to passive initialization. This feedback cools the transmon from a spurious steady-state excitation of 16% to 3% and resets qubit states with 2.4% error averaged over the Bloch sphere. These absolute errors are dominated by latency, in quantitative agreement with a model including transmon equilibration and readout errors.

The experiment employs a transmon qubit inside an aluminum 3D cavity [13]. The qubit ($\omega_{01}/2\pi = 4.889$ GHz transition frequency) couples to the cavity fundamental mode ($\omega_\mathrm{r}/2\pi = 6.546$ GHz, coupling-limited linewidth $\kappa/2\pi = 550$ kHz) with strength $g/2\pi = 68$ MHz. The high-fidelity, projective qubit readout forming the input to the feedback loop uses homodyne detection of the qubit-state dependent cavity transmission (dispersive shift $2\chi/2\pi = -1.9$ MHz [12]). A 400 ns measurement pulse at $\omega_\mathrm{m} = \omega_\mathrm{r} - \chi$ is applied to the cavity and the transmitted signal is then amplified by a Josephson parametric amplifier [14, 15] to enhance detection sensitivity, as developed in Refs. 16 and 17. The feedback controller, closing the loop between qubit measurement and control, is an ADwin Gold processor that samples the transmitted homodyne signal, performs 1-bit digitization to interpret the projected qubit state, and conditionally triggers a π pulse resonant with the transmon $0 \leftrightarrow 1$ transition. The 2.64 μs delay between start of the measurement and end of the π pulse, set by processing time in the ADwin, is short compared to the qubit relaxation time T_1 (see below) [22].

Our first application of feedback is qubit initialization, also known as reset [7]. The ideal reset for QIP is deterministic (as opposed to heralded or postselected [16, 17]) and fast compared to qubit coherence times. Obviously, the passive method of waiting several times T_1 does not meet the speed requirement. Moreover, it can suffer from residual steady-state qubit excitations [16–18, 23], whose cause in cQED remains an active research area. The drawbacks of passive initialization are evident for our qubit, whose ground-state population $P_{|0\rangle}$ evolves from states ρ_0 and ρ_1 as shown in Fig. 1. With ρ_0 and ρ_1 we indicate our closest realization ($\sim 99\%$ fidelity) of the ideal pure states $|0\rangle$ and $|1\rangle$ (see below and Ref. 16). $P_{|0\rangle}$ at variable time after preparation is obtained by comparing the average readout homodyne voltage to calibrated levels [24], as in standard three-level tomography [25, 26].
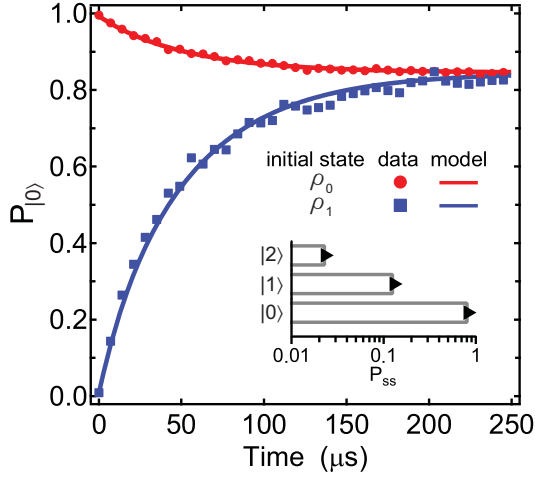
FIG. 1. (color online). Transmon equilibration to steady state. Time evolution of the ground-state population $P_{|0\rangle}$ starting from states ρ_0 and ρ_1 (notation defined in the text). Solid curves are the best fit (including data in Fig. S4) to Eq. (1), giving the inverse transition rates $\Gamma_{01}^{-1} = 50 \pm 2\ \mu s$, $\Gamma_{12}^{-1} = 20 \pm 2\ \mu s$, $\Gamma_{10}^{-1} = 324 \pm 32\ \mu s$, $\Gamma_{21}^{-1} = 111 \pm 25\ \mu s$. From the steady-state solution, we extract residual excitations $P_{|1\rangle,ss} = 13.1 \pm 0.8\%$, $P_{|2\rangle,ss} = 2.4 \pm 0.4\%$. Inset: steady-state population distribution (bars). Markers correspond to a Boltzmann distribution with best-fit temperature 127 mK, significantly higher than the dilution refrigerator base temperature (15 mK).

These populations dynamics are captured by a master equation model for a three-level system:

$$\begin{pmatrix} \dot{P}_{|0\rangle} \\ \dot{P}_{|1\rangle} \\ \dot{P}_{|2\rangle} \end{pmatrix} = \begin{pmatrix} -\Gamma_{10} & \Gamma_{01} & 0 \\ \Gamma_{10} & -\Gamma_{01} - \Gamma_{21} & \Gamma_{12} \\ 0 & \Gamma_{21} & -\Gamma_{12} \end{pmatrix} \begin{pmatrix} P_{|0\rangle} \\ P_{|1\rangle} \\ P_{|2\rangle} \end{pmatrix}.$$

(1)

The best fit to the data gives the qubit relaxation time $T_1 = 1/\Gamma_{01} = 50 \pm 2\ \mu s$ and the asymptotic 15.5% residual total excitation.

Previous approaches to accelerate qubit equilibration include coupling to dissipative resonators [27] or two-level systems [28]. However, these are also susceptible to spurious excitation, potentially inhibiting complete qubit relaxation. Feedback-based reset circumvents the equilibration problem by not relying on coupling to a dissipative medium. Rather, it works by projecting the qubit with a measurement (M_1, performed by the controller) and conditionally applying a π pulse to drive the qubit to a targeted basis state (Fig. 2). A final measurement (M_2) determines the qubit state immediately afterwards. In both measurements, the result is digitized into levels H or L, associated with $|0\rangle$ and $|1\rangle$, respectively. The digitization threshold voltage V_{th} maximizes the readout fidelity at 99%. The π pulse is conditioned on $M_1 = L$ to target $|0\rangle$ (scheme Fb$_0$) or on $M_1 = H$ to target $|1\rangle$ (Fb$_1$). In a QIP context, reset is typically used to reinitialize a qubit following measurement, when it is in a computa-
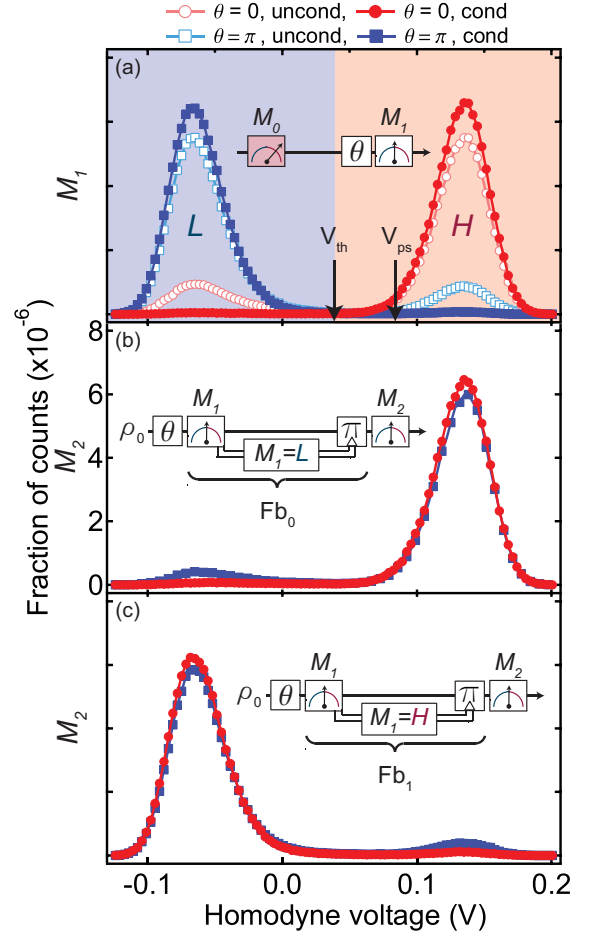

FIG. 2. (color online). Reset by measurement and feedback. (a) Before feedback: histograms of 300 000 shots of M_1, with (squares) and without (circles) inverting the qubit population with a π pulse. Each shot is obtained by averaging the homodyne voltage over the second half (200 ns) of a readout pulse. H and L denote the two possible outcomes of M_1, digitized with the threshold V_{th}, maximizing the contrast, analogously to Ref. 16. Full (empty) dots indicate (no) postselection on $M_0 > V_{ps}$. This protocol [24] is used to prepare ρ_0 and ρ_1, which are the input states for the feedback sequences in (b) and (c). (b) After feedback: histograms of M_2 after applying the feedback protocol Fb$_0$, which triggers a π pulse when $M_1 = L$. Using this feedback, $\sim 99\%$ (92%) of measurements digitize to H for $\theta = 0$ (π), respectively. (c) Feedback with opposite logic Fb$_1$ preparing the excited state. In this case, $\sim 98\%$ (94%) of measurements digitize to L for $\theta = 0$ (π).

tional basis state. Therefore, to benchmark the reset protocol, we first quantify its action on ρ_0 and ρ_1. This step is accomplished with a preliminary measurement M_0 (initializing the qubit in ρ_0 by postselection [16, 17, 24]), followed by a calibrated pulse resonant on the transmon $0 \leftrightarrow 1$ transition to prepare ρ_1. The overlap of the M_2 histograms with the targeted region (H for Fb$_0$ and L for Fb$_1$) averages at 96%, indicating the success of reset. Imperfections are more evident for $\theta = \pi$ and mainly due to equilibration of the transmon during the feedback
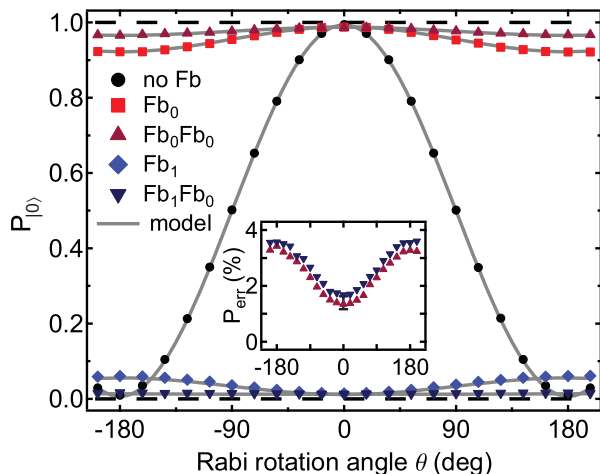
FIG. 3. (color online). Deterministic reset from any qubit state. Ground-state population $P_{|0\rangle}$ as a function of the initial state ρ_θ, prepared by coherent rotation after initialization in ρ_0, as in Fig. 2. The cases shown are: no feedback (circles), Fb_0 (squares), Fb_1 (diamonds), twice Fb_0 (upward triangles), and Fb_0 followed by Fb_1 (downward triangles). The vertical axis is calibrated with the average measurement outcome for the reference states ρ_0, ρ_1, and corrected for imperfect state preparation [24]. The curve with no feedback has a visibility of 99%, equal to the average preparation fidelity. Each experiment is averaged over 300 000 repetitions. Inset: error probabilities for two rounds of feedback, defined as $1 - P_{|t\rangle}$, where $|t\rangle \in \{0, 1\}$ is the target state. The systematic $\sim 0.3\%$ difference between the two cases is attributed to error in the π pulse preceding the measurement of $P_{|1\rangle}$ following Fb_1 [24]. Curves: model including readout errors and equilibration [24].

loop. A detailed error analysis is presented below. We emphasize that qubit initialization by postselection (an inherently probabilistic method demonstrated in Refs. 16 and 17) is here only used to prepare nearly pure states useful for characterizing the feedback-based reset, which is deterministic.

An ideal reset function prepares the same pure qubit state regardless of its input. To fully quantify the performance of our reset scheme, we measure its effect on our closest approximation to superposition states $|\theta\rangle = \cos(\theta/2)|0\rangle + \sin(\theta/2)|1\rangle$. Without feedback, $P_{|0\rangle}$ is trivially a sinusoidal function of θ, with near unit contrast. Feedback highly suppresses the Rabi oscillation, with $P_{|0\rangle}$ approaching the ideal value 1 (0) for Fb_0 (Fb_1) for any input state. However, a dependence on θ remains, with $P_{\text{err}} = 1 - P_{|0\rangle}$ for Fb_0 ($1 - P_{|1\rangle}$ for Fb_1) ranging from 1.2% (1.4%) for $\theta = 0$ to 7.8% (8.4%) for $\theta = \pi$. The remaining errors have two sources: mismatch between measurement result M and post-measurement state $|i\rangle$, occurring with probability p_{ij}^M, for initial state $|j\rangle$; and equilibration during the $\tau = 2.4$ μs lapse between the end of M_1 and the start of M_2, set by processing time in the controller. Transitions to $|2\rangle$ during M_1 (with probability $p_{21} = p_{21}^H + p_{21}^L$), or during τ ($\Gamma_{21}\tau$), cause leakage
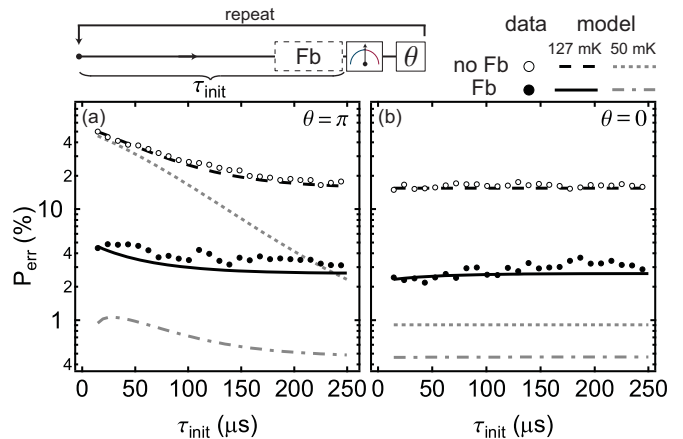

FIG. 4. (color online). Fast qubit reset. Initialization errors as a function of initialization time τ_{init} under looped execution of a simple experiment leaving the qubit ideally in $|1\rangle$ [(a), measurement and π pulse] or $|0\rangle$ [(b), measurement only]. Empty circles: initialization by waiting (no feedback). Solid dots: initialization by feedback, with three rounds of Fb_0 and a π pulse on the $1 \leftrightarrow 2$ transition [24]. Curves correspond to a master equation simulation assuming perfect pulses and either the measured transition rates Γ_{ij} (dashed, no feedback; solid, triple Fb_0 with a π pulse on $1 \leftrightarrow 2$) or the calculated [29] rates for 50 mK (dotted, no feedback; dot-dashed, triple Fb_0). Feedback reset successfully bounds the otherwise exponential accruement of P_{err} in case (a) as $\tau_{\text{init}} \to 0$. The reduction of P_{err} in (b) reflects the cooling of the transmon by feedback (see text for details).

out of the qubit subspace, where the feedback has no action. For perfect pulses, the overall errors (equal for Fb_0 and Fb_1) are to first order:

$$
\begin{aligned}
P_{\text{err}}^{\theta=0} &= p_{00}^L + p_{10}^H + \Gamma_{10}\tau, \\
P_{\text{err}}^{\theta=\pi} &= p_{11}^H + p_{01}^L + p_{21} + (\Gamma_{01} + \Gamma_{21})\tau,
\end{aligned}
\tag{2}
$$

and weighted combinations thereof for other θ. Using the best-fit Γ_{ij}, errors due to equilibration sum to 0.7% (6.9%) for $\theta = 0$ (π), while readout errors account for the remaining 0.4% (1.4%).

A simple way to improve reset fidelity is to concatenate two feedback cycles. While the dominant error for $\theta = 0$ remains unchanged, for $\theta = \pi$ it decreases to $P_{\text{err}}^{\theta=0} + p_{21} + \Gamma_{21}\tau$, in agreement with the measured values of 1.3% and 3.4%, respectively. The second cycle compensates errors arising from relaxation to $|0\rangle$ between measurement and pulse in the first cycle. However, it does not correct for excitation from $|1\rangle$ to $|2\rangle$. For this reason, adding more cycles does not significantly reduce the error, unless the population in $|2\rangle$ is brought back to the qubit subspace, as shown below. Further improvement may be achieved by decreasing τ, for example by using field-programmable gate arrays for faster processing.

The key advantage of reset by feedback is the ability to ready a qubit for further computation fast compared to coherence times available in 3D cQED [13, 30]. This

will be important, for example, when refreshing ancilla qubits in multi-round error correction [31]. We now show that reset suppresses the accumulation of initialization error when a simple experiment is repeated with decreasing in-between time τ_{init}. The simple sequence in Fig. 4 emulates an algorithm that leaves the qubit in $|1\rangle$ [case (a)] or $|0\rangle$ [case (b)]. A measurement pulse follows τ_{init} to quantify the initialization error P_{err}. Without feedback, P_{err} in case (a) grows exponentially as $\tau_{\text{init}} \to 0$. This accruement of error, due to the rapid succession of π pulses, would occur even at zero temperature, where residual excitation would vanish (i.e., $\Gamma_{i+1,i} = 0$), in which case $P_{\text{err}} \to 50\%$ as $\tau_{\text{init}} \to 0$. In case (b), P_{err} matches the total steady-state excitation for all τ_{init}. Using feedback significantly improves initialization for both long and short τ_{init}. For $\tau_{\text{init}} \gg T_1$, feedback suppresses P_{err} from the 16% residual excitation to 3% [32], cooling the transmon. Crucially, unlike passive initialization, reset by feedback is also effective at short τ_{init}, where it limits the otherwise exponential accruement of error in (a), bounding P_{err} to an average of 3.5% over the two cases. Our scheme combines three rounds of Fb_0 with a pulse on the $1 \leftrightarrow 2$ transition before the final Fb_0 to partially counter leakage to the second excited state [24], which is the dominant error source [see Eq. (2)]. The remaining leakage is proportional to the average $P_{|1\rangle}$, which slightly increases in (a) and decreases in (b) as $\tau_{\text{init}} \to 0$. For 50 mK, we estimate that, with Γ_{21} being suppressed, fast reset will constrain $P_{\text{err}} \leq 1\%$ (Fig. 4), quoted as the fault-tolerance threshold for initialization in modern error correction schemes [33]. Such a moderate temperature reduction may be achieved by a combination of radiation shielding [23], use of a copper cavity [34], and improved qubit thermal anchoring.

In conclusion, we have demonstrated feedback control of a transmon qubit using high-fidelity projective measurement and conditional operation. We have applied this feedback to deterministically reset the qubit, starting from any superposition, with 2.4% average error. We have also demonstrated that feedback-based initialization is fast compared to the passive method. While this demonstration employs feedback on a single qubit, the scheme can be extended to conditionally drive a different qubit than the one measured, realizing the feedforward [1] needed for teleportation and measurement-based error correction. Future experiments will also target the generation of entanglement by combining this feedback scheme with cavity-based parity measurements [35, 36] and the observation of quasiparticle tunneling in transmon qubits in real time using fast reset. The latter may shine light on a decoherence mechanism of current theoretical [37] and experimental [38, 39] interest.

Note added.—A parallel manuscript from École Normale Supérieure, Paris [40] reports feedback control of a transmon qubit using a Josephson parametric converter for high-fidelity projective readout.

———

[1] H. M. Wiseman and G. J. Milburn, *Quantum measurement and control* (Cambridge University Press, Cambridge, 2009).
[2] M. A. Nielsen and I. L. Chuang, *Quantum Computation and Quantum Information* (Cambridge University Press, Cambridge, 2000).
[3] J. Chiaverini, *et al.*, Nature **432**, 602 (2004).
[4] M. Riebe, *et al.*, Nature **429**, 734 (2004).
   M. D. Barrett, *et al.*, Nature **429**, 737 (2004).
[5] T. B. Pittman, B. C. Jacobs, and J. D. Franson, Phys. Rev. A **71**, 052332 (2005).
[6] A. Furusawa, J. L. Sørensen, S. L. Braunstein, C. A. Fuchs, H. J. Kimble, and E. S. Polzik, Science **282**, 706 (1998).
[7] D. P. DiVincenzo, Fortschritte der Physik **48**, 771 (2000).
[8] J. Clarke and F. K. Wilhelm, Nature **453**, 1031 (2008).
[9] L. DiCarlo, *et al.*, Nature **460**, 240 (2009).
   T. Yamamoto, *et al.*, Phys. Rev. B **82**, 184515 (2010).
   A. Dewes, R. Lauro, F. R. Ong, V. Schmitt, P. Milman, P. Bertet, D. Vion, and D. Esteve, Phys. Rev. B **85**, 140503 (2012).
   E. Lucero, *et al.*, Nature Phys. **8**, 719 (2012).
[10] M. Baur, A. Fedorov, L. Steffen, S. Filipp, M. P. da Silva, and A. Wallraff, Phys. Rev. Lett. **108**, 040502 (2012).
[11] A. Blais, R.-S. Huang, A. Wallraff, S. M. Girvin, and R. J. Schoelkopf, Phys. Rev. A **69**, 062320 (2004).
[12] A. Wallraff, D. I. Schuster, A. Blais, L. Frunzio, R.-S. Huang, J. Majer, S. Kumar, S. M. Girvin, and R. J. Schoelkopf, Nature **431**, 162 (2004).
[13] H. Paik, *et al.*, Phys. Rev. Lett. **107**, 240501 (2011).
[14] M. A. Castellanos-Beltran, K. D. Irwin, G. C. Hilton, L. R. Vale, and K. W. Lehnert, Nature Phys. **4**, 929 (2008).
[15] R. Vijay, M. H. Devoret, and I. Siddiqi, Rev. Sci. Instrum. **80**, 111101 (2009).
[16] D. Ristè, J. G. van Leeuwen, H.-S. Ku, K. W. Lehnert, and L. DiCarlo, Phys. Rev. Lett. **109**, 050507 (2012).
[17] J. E. Johnson, C. Macklin, D. H. Slichter, R. Vijay, E. B. Weingarten, J. Clarke, and I. Siddiqi, Phys. Rev. Lett. **109**, 050506 (2012).
[18] R. Vijay, C. Macklin, D. H. Slichter, K. W. Murch, R. Naik, N. Koroktov, and I. Siddiqi, Nature **490**, 77 (2012).
[19] G. G. Gillett, *et al.*, Phys. Rev. Lett. **104**, 080503 (2010).
   C. Sayrin, *et al.*, Nature **477**, 73 (2011).
[20] P. Bushev, *et al.*, Phys. Rev. Lett. **96**, 043003 (2006).
[21] M. Koch, C. Sames, A. Kubanek, M. Apel, M. Balbach, A. Ourjoumtsev, P. W. H. Pinkse, and G. Rempe, Phys. Rev. Lett. **105**, 173003 (2010).
   S. Brakhane, W. Alt, T. Kampschulte, M. Martinez-

Dorantes, R. Reimann, S. Yoon, A. Widera, and D. Meschede, Phys. Rev. Lett. **109**, 173601 (2012).

[22] The Ramsey dephasing time $T_2^* = 2$ μs is most likely due to photon shot noise [41] and sensitivity to charge noise due to the low ratio $E_J/E_C \sim 27$ [42]. Dephasing is however not relevant for the reset application here demonstrated.

[23] A. D. Córcoles, J. M. Chow, J. M. Gambetta, C. Rigetti, J. R. Rozen, G. A. Keefe, M. Beth Rothwell, M. B. Ketchen, and M. Steffen, Appl. Phys. Lett. **99**, 181906 (2011).

[24] See supplemental material for details on feedback setup, measurement of the transmon populations, readout model and comparison of feedback protocols.

[25] R. T. Thew, K. Nemoto, A. G. White, and W. J. Munro, Phys. Rev. A **66**, 012303 (2002).

[26] R. Bianchetti, S. Filipp, M. Baur, J. M. Fink, M. Göppl, P. J. Leek, L. Steffen, A. Blais, and A. Wallraff, Phys. Rev. A **80**, 043840 (2009).

[27] M. D. Reed, B. R. Johnson, A. A. Houck, L. DiCarlo, J. M. Chow, D. I. Schuster, L. Frunzio, and R. J. Schoelkopf, Appl. Phys. Lett. **96**, 203110 (2010).

[28] M. Mariantoni, *et al.*, Science **334**, 61 (2011).

[29] A. Palacios-Laloy, F. Mallet, F. Nguyen, F. Ong, P. Bertet, D. Vion, and D. Esteve, Phys. Scr. **T137**, 014015 (2009).

[30] C. Rigetti, *et al.*, Phys. Rev. B **86**, 100506 (2012).

[31] P. Schindler, J. T. Barreiro, T. Monz, V. Nebendahl, D. Nigg, M. Chwalla, M. Hennrich, and R. Blatt, Science **332**, 1059 (2011).

[32] We note that $P_{|1\rangle} \approx P_{|2\rangle} = 1.6\%$ is a non-thermal distribution.

[33] D. S. Wang, A. G. Fowler, and L. C. L. Hollenberg, Phys. Rev. A **83**, 020302 (2011).

[34] We have recently measured a residual excitation of $\sim 2\%$ for a qubit at the same frequency inside a Cu cavity of the same geometry, consistent with Ref. 30.

[35] K. Lalumière, J. M. Gambetta, and A. Blais, Phys. Rev. A **81**, 040301 (2010).

[36] L. Tornberg and G. Johansson, Phys. Rev. A **82**, 012329 (2010).

[37] G. Catelani, R. J. Schoelkopf, M. H. Devoret, and L. I. Glazman, Phys. Rev. B **84**, 064517 (2011).

[38] L. Sun, *et al.*, Phys. Rev. Lett. **108**, 230509 (2012).

[39] M. Lenander, *et al.*, Phys. Rev. B **84**, 024501 (2011).

[40] P. Campagne-Ibarcq, *et al.*, in preparation (2012).

[41] A. P. Sears, *et al.*, arXiv:1206.1265.

[42] J. A. Schreier, *et al.*, Phys. Rev. B **77**, 180502 (2008).